# Structure and properties of poly(ethylene terephthalate) crystallized by annealing in the highly oriented state: 2. Melting behaviour and the mosaic block structure of the crystalline layers

**S. Fakirov*, E. W. Fischer†, R. Hoffmann and G. F. Schmidt**
*Institut fur Physikalische Chemie der Universitat Mainz, 6500 Mainz, W. Germany and 'Sonderforschungsbereich 41', Mainz/Darmstadt, W. Germany*
*(Received 14 August 1976; revised 19 May 1977)*

The melting behaviour of drawn poly(ethylene terephthalate) bristles has been studied by means of differential scanning calorimetry. In addition the wide-angle X-ray diffraction pattern were analysed. For comparison some of the experiments were also carried out with undrawn samples. The differences in the melting curves of drawn and undrawn PET originate from the different crystallization kinetics. The density defect ($\rho_c^{id} - \rho_c^*$) between the ideal crystal density $\rho_c^{id}$ and the effective density $\rho_c^*$ of the crystalline layers is a result of lattice vacancies introduced by the grain boundaries of the mosaic blocks. The relatively low ultimate crystallinity of PET is supposed to be caused by the hindrance of crystal growth of fibre direction during isothermal crystallization.

## INTRODUCTION

Poly(ethylene terephthalate) (PET) quenched from the melt and subsequently drawn in the amorphous state can be crystallized by annealing at temperatures above the glass transition. The dependence of the structure of the semicrystalline samples on the annealing conditions has been studied mainly by means of small-angle X-ray scattering (SAXS). The results were reported in part 1 of this paper[1]. In addition the melting behaviour, the wide-angle X-ray scattering, and the mechanical properties of those samples were investigated.

This paper is concerned mainly with the analysis of the melting curves obtained by differential scanning calorimetry (d.s.c.), with the determination of the apparent crystallite sizes, and with the discussion of a structure model for the crystalline layers in the semicrystalline oriented PET. The mechanical behaviour will be described in part 3.

In part 1 it was concluded that the effective density $\rho_c^*$ of the crystalline layers is considerably less than the ideal value $\rho_c^{id}$ derived from the unit cell parameters measured by wide-angle X-ray scattering. For the calculations a 'crystallinity index' was used based on the measured heat of fusion. These measurements are now discussed in more detail. In addition wide-angle X-ray scattering studies were performed in order to verify the structure model which we developed from the results of SAXS measurements.

## EXPERIMENTAL

### *Samples*

The same samples were used as for the SAXS measurements described in part 1. Amorphous PET bristles of 1 mm thickness were drawn about 5 times at 65°C and subsequently annealed with fixed ends at various temperatures. For comparison undrawn material was also studied. A more detailed description of sample preparation is given in ref 1.

### *D.s.c. measurements*

A Du Pont Differential Thermal Analyzer model 990, was used for the experiments. The analysis was carried out in an air atmosphere with specimens of ~5 mg. The effect of heating rate due to the time lag of the apparatus was determined and the data for the melting temperature were accordingly corrected. In many cases this effect was small compared with the influence of reorganization processes (see *Figure 5*). The peak areas of the d.s.c. curves were determined by drawing a base line as indicated for example in *Figure 3*. In cases where a double melting peak appeared the peak areas were determined separately.

From the measured heat of fusion $\Delta H_{exp}$ an apparent degree of crystallinity $w_c$ (d.s.c.) was determined according to:

$$w_c(\text{d.s.c.}) = \frac{\Delta H_{exp}}{\Delta H^\circ} \qquad (1)$$

where $\Delta H^\circ$ is the heat of fusion (per mole of repeating unit) of an ideal PET crystal.

As is well known the crystallinity values obtained from equation (1) are subject to various uncertainties:

(a) The enthalpy change $\Delta H^\circ$ during melting of an ideal PET crystal is not known exactly. We adopted the value of 5.8 kcal/mol = 24.3 kJ/mol given by Wunderlich[2], which is close to those proposed by other authors[3].

(b) In equation (1) the effect of the surface energy is

* Present address: University of Sofia, Faculty of Chemistry, Sofia 26, Bulgaria.
† Present address: Department of Physics, University of Leeds, UK.

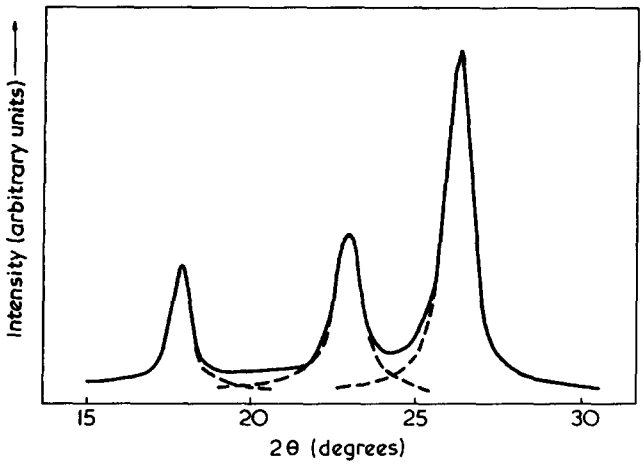


*Figure 1* Equatorial X-ray diffraction pattern of drawn PET annealed at 255°C. — — —, were used for determination of the line width at half-maximum intensity

neglected. In the case of a lamellar crystal with thickness $l$ the measured heat of fusion $\Delta H_{exp}$ has to be corrected by:

$$\Delta H_\infty = \Delta H_{exp} + \frac{2\sigma_e w_c v_c}{l} \quad (2)$$

where $\sigma_e$ is the surface energy of the lamellae; the lateral surfaces are not taken into account. Generally this correction amounts to very few cal/g and is therefore in the range of variance of $\Delta H^\circ$.

(c) The crystallinity $w_c$ (d.s.c.) determined by equation (1) measures the weight fraction of crystalline material, whereas in connection with the evaluation of SAXS data the volume fraction crystallinity is used. We believe that the small difference is compensated by the grain boundary surface energy of the mosaic blocks (see below).

(d) During the d.s.c. run of a drawn polymer the sample is subjected to shrinkage and disorientation. The influence of these processes on the measured values of $\Delta H_{exp}$ is not known; in the case of polyethylene only small effects were found[6]. All these effects may influence the values of $w_c$ (d.s.c.), the largest error is probably due to the inaccuracy of $\Delta H^\circ$. For a low molecular weight PET of high crystallinity a value of 6.2 kcal/mol has been found by Illers[22]. A somewhat higher value than 5.8 kcal/mol used in our work may also be justified by the fact, that some of the earlier work[3] is based on comparison with density data using a lower value of $\rho_c^{id}$ than we did[1]. So the absolute values of $w_c$ (d.s.c.) are subjected to this uncertainty, which is not relevant, however, with regard to our structure model.

*Determination of apparent crystallite sizes*

The wide-angle X-ray scattering of the drawn samples was measured by a counter diffractometer using Ni-filtered CuKα radiation detected by a scintillation counter with single-channel discrimination. The instrumental broadening was negligibly small compared with the width of the reflection peaks. The separation of the reflections was carried out under the assumption of symmetrical line shape (see *Figure 1*). The reflection shape was characterized by the breadth $\Delta_{hkl}$ at half-maximum intensity and an apparent crystallite size $D_{hkl}$ was calculated[7] from the Scherrer equation:

$$D_{hkl} = \frac{0.89\lambda}{\Delta_{hkl}\cos\theta} \quad (3)$$

As is well known this value leads to a lower limit of the real crystallite size since the broadening of the reflections can also be due to lattice distortions. For reasons which we discussed in part 1, we suppose the main source of broadening to be the crystallite size. For one sample the line width of the 1st and 2nd order of the 100-reflection was also measured. They do not quite coincide but an analysis according to Hosemann's procedure[8] gives a correction of only about 15% which has no significance with regard to the conclusions drawn from the discussion below.

## RESULTS AND DISCUSSION

*Appearance of double melting peaks*

The d.s.c. fusion curves of some of the investigated samples are plotted in *Figures 2* and *3*. Within a certain range of annealing temperatures the appearance of two fusion endotherms is observed. There exists characteristic differences between the behaviour of drawn and undrawn PET, as was also shown by Yubayashi *et al.*[9]. For given annealing temperatures and annealing times the first melting peak $T'_m$ is located at much lower temperatures for undrawn than for drawn samples. In addition the position of $T'_m$ for drawn PET does not depend on the annealing temperature $T_a$ in contrast to the behaviour of undrawn samples. This is demonstrated by *Figure 4*. The experimental data of all samples investigated are summarized in *Tables 1* and *2*.

First we discuss the characteristic features of the melting curves in the case of undrawn material. In this case the occurrence of two endothermic maxima in the d.s.c. thermo-

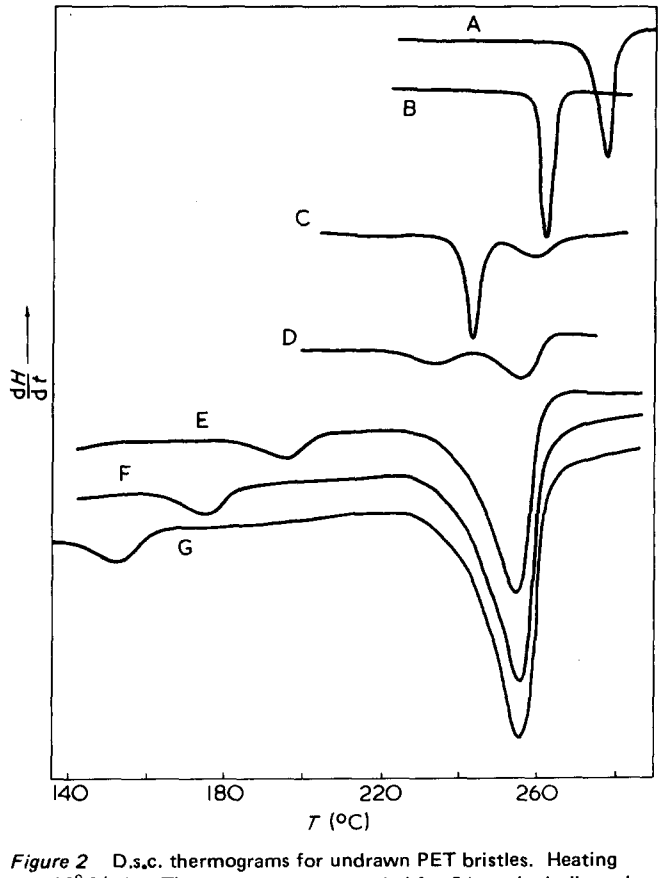


*Figure 2* D.s.c. thermograms for undrawn PET bristles. Heating rate 10°C/min. The samples were annealed for 6 h at the indicated temperatures. A, 260°C; B, 240°C; C, 220°C; D, 200°C; E, 180°C; F, 160°C; G, 140°C

grams has been observed already by many investigators[10,11] (for earlier literature references see ref 11). In general accordance with these studies we also found that the temperature position of the second melting peak $T_m''$ remains constant over a large range of annealing temperatures $T_a$ (140° to 240°C), whereas the first melting peak $T_m'$ depends strongly on $T_a$ and is usually found to be 15°–20°C above the annealing temperature after an annealing time of 6 h. With rising $T_a$ the integrated area of the first peak ($\Delta H'$) increases at the expense of the second peak ($\Delta H''$) and only small changes of the overall heat of fusion $\Delta H = \Delta H' + \Delta H''$ are observed (see *Tables 1* and *2*).

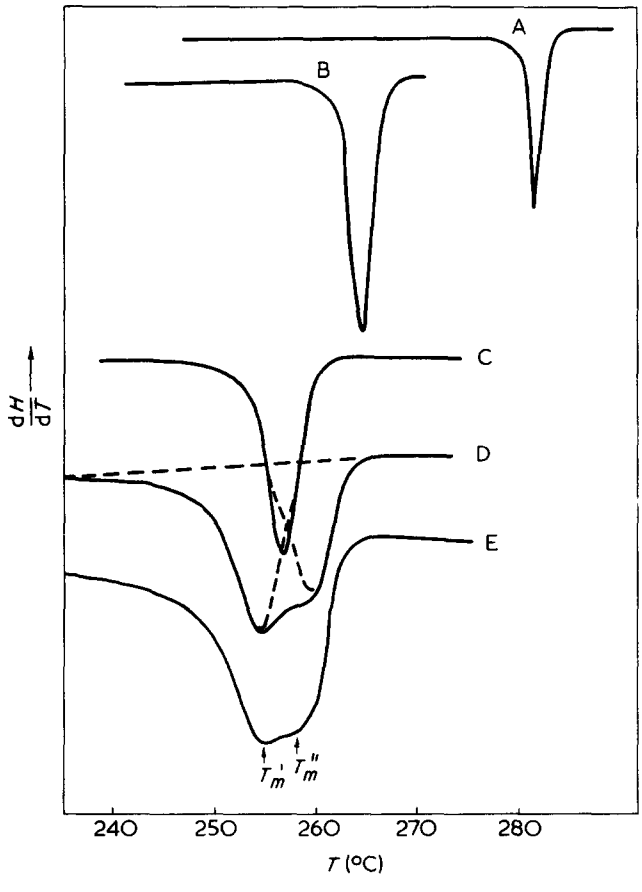


*Figure 3* D.s.c. thermograms for PET bristles drawn about 5 X. Heating rate and annealing times as in *Figure 2*. A, 260°C; B, 240°C; C, 220°C; D, 180°C; E, 140°C

When discussing the origin of the multiple melting endotherms it is important to study the dependence of the fusion curves on the heating rate during the d.s.c. measurements. Two samples were chosen (annealing temperatures 160° and 220°C) which both show two distinct peaks but differ with regard to the relative areas $\Delta H'/\Delta H$. The temperature positions of the two peaks $T_m'$ and $T_m''$ are plotted in *Figure 5*. For both samples an increase of $T_m'$ and a decrease of $T_m''$ is observed dependent on heating rate. A qualitatively similar behaviour has been observed by Illers *et al.*[5] in the case of polyamide-6.

The described fusion curves indicate a characteristic behaviour of semicrystalline polymers, which undergo a continuous reorganization during the d.s.c. scan. As it was pointed out by Holdsworth *et al.*[11] the two endothermic peaks observed during the melting of PET can be explained on the basis of the assumption, that crystallites formed at low temperatures melt and recrystallize with a higher perfection during the scan. This explanation does not necessarily imply that the crystallites melt completely, there may exist

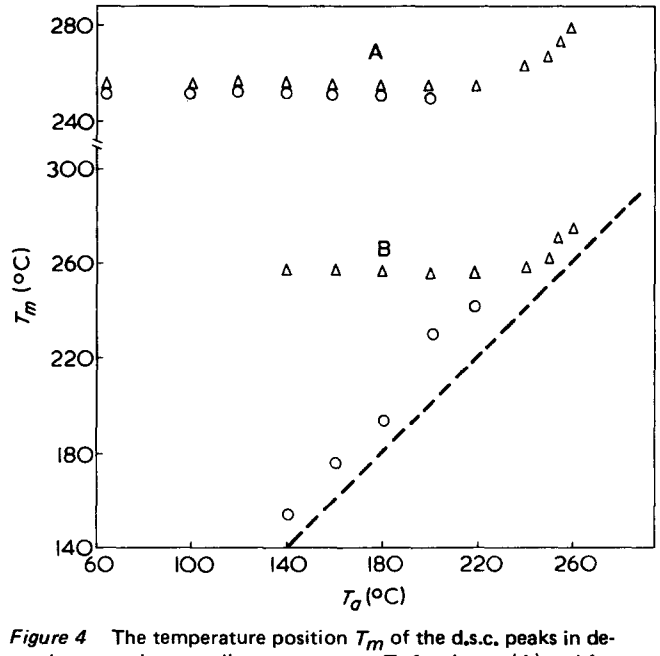


*Figure 4* The temperature position $T_m$ of the d.s.c. peaks in dependence on the annealing temperature $T_a$ for drawn (A) and for isotropic (B) PET samples. ○, first d.s.c. peak $T_m'$; △, second peak $T_m''$. – – –, indicates $T_m = T_a$

*Table 1* Calorimetric data for PET bristles in the undrawn state

| Annealing temperatures, $T_a$ (°C) | $T_m'$ (°C) | $T_m''$ (°C) | $\Delta H'$ (cal/g) | $\Delta H''$ (cal/g) | $\Delta H = \Delta H' + \Delta H''$ (cal/g) | $w_c$ from d.s.c. | $w_c$ from $\rho$ |
|---|---|---|---|---|---|---|---|
| Unannealed | – | – | – | – | – | – | 0.03 |
| 100 | – | – | – | – | – | – | 0.13 |
| 120 | – | – | – | – | – | – | 0.20 |
| 140 | 154 | 256 | 0.8 | 8.3 | 9.0 | 0.33 | 0.23 |
| 160 | 175 | 256 | 0.8 | 9.3 | 10.2 | 0.35 | 0.25 |
| 180 | 193 | 256 | 0.5 | 9.2 | 10.6 | 0.36 | 0.30 |
| 200 | 230 | 255 | 2.7 | 6.8 | 9.5 | 0.36 | 0.33 |
| 220 | 242 | 254 | 7.4 | 3.3 | 10.6 | 0.36 | 0.39 |
| 240 | 257 | | 12.9 | | 12.9 | 0.44 | 0.48 |
| 250 | 262 | | 12.4 | | 12.4 | 0.42 | 0.46 |
| 255 | 270 | | 13.7 | | 13.7 | 0.45 | 0.43 |
| 260 | 275 | | 10.0 | | 10.0 | 0.34 | 0.36 |

*Table 2* Calorimetric data for PET bristles in the drawn state

| Annealing temperatures, $T_a$ (°C) | $T'_m$ (°C) | $T''_m$ (°C) | $\Delta H'$ (cal/g) | $\Delta H''$ (cal/g) | $\Delta H = \Delta H' + \Delta H''$ (cal/g) | $w_c$ from d.s.c. | $w_c$ from $\rho$ |
|---|---|---|---|---|---|---|---|
| Unannealed | – | – | – | – | – | – | 0.13 |
| 100 | 252 | 255 | 8.3 | 4.7 | – | – | 0.23 |
| 120 | 251 | 255 | 8.2 | 4.3 | – | – | 0.22 |
| 140 | 251 | 255 | 7.5 | 4.6 | 12.1 | 0.41 | 0.26 |
| 160 | 251 | 255 | 8.3 | 4.7 | 13.0 | 0.45 | 0.30 |
| 180 | 251 | 255 | 7.5 | 4.3 | 11.8 | 0.41 | 0.35 |
| 200 | 252 | 255 | 9.1 | 4.6 | 13.7 | 0.47 | 0.43 |
| 220 | 254 | | 14.5 | | 14.5 | 0.49 | 0.53 |
| 240 | 262 | | 15.5 | | 15.5 | 0.53 | 0.56 |
| 250 | 268 | | 15.6 | | 15.6 | 0.53 | 0.56 |
| 255 | 273 | | 14.3 | | 14.3 | 0.48 | 0.54 |
| 260 | 277 | | 11.3 | | 11.3 | 0.39 | 0.40 |

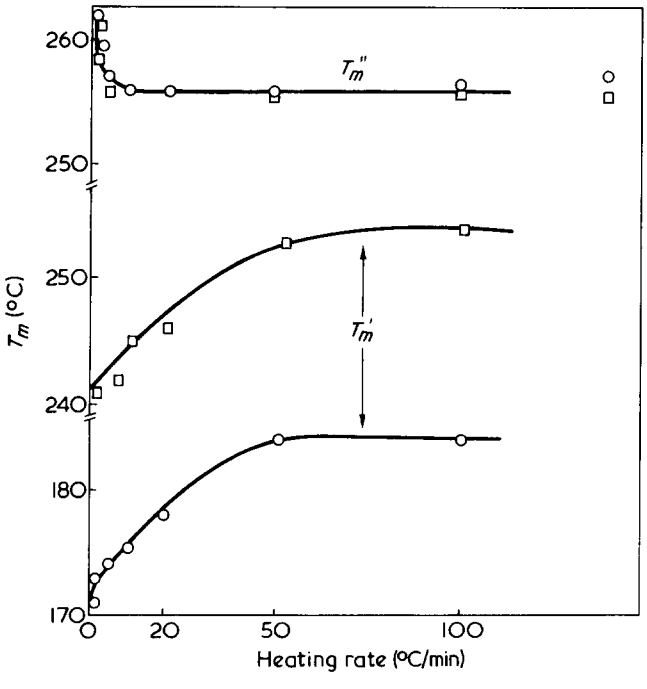


*Figure 5* Peak positions $T'_m$ and $T''_m$ of undrawn PET in dependence on heating rate during the d.s.c. scan. The samples were annealed at 160° or 220°C respectively. ○, $T_a$ = 160° C; □, $T_a$ = 220°C

some type of internal reorganization process which leads to a higher perfection. The 'superheating' effect observed for $T'_m$ (see *Figure 5*) may be either due to slow melting of the original crystals or – more likely – due to a broad melting point distribution of those crystals. In such a case the observed melting peak $T'_m$ is determined by the two competitive processes of melting and recrystallization. For fast heating rates no recrystallization takes place and the position of the maximum of the melting peak is only determined by the shape of the melting point distribution curve. In the case of low heating rates, however, the measured curve is due to the sum of endothermic melting and exothermic recrystallization and therefore the melting of the larger crystals is overlapped by the crystallization heat. So the observed position of the maximum depends not only on the melting point distribution curve but also on the ratio between heating and recrystallization rate.

For a complete description of the origin of the double peak a careful analysis of the small-angle X-ray pattern's dependence on heating history seems to be important. Such a study is now undertaken and the results will be reported later. Presently we have no indications that the conclusions drawn by Holdsworth *et al.*[11] must be changed in principle.

Now we turn to the behaviour of drawn material. As it was pointed out already there exists characteristic differences between the fusion curves of drawn and undrawn PET (see *Figures 2–4*). The first peak $T'_m$ is located at higher temperatures and the area beneath this peak is much larger. At temperatures below 240°C no peak is found as is the case in undrawn material. A similar behaviour for polyamide-6,6 has been already observed by Bell and Dumbleton[12] and has been interpreted as a 'conversion from material represented by a higher temperature endotherm to material represented by a lower temperature endotherm taking place during cold drawing'. The conclusion drawn by these authors is that the first type of material consists of crystals in which the chains are folded the second (lower melting) type contains crystals in which the chains within the crystals are extended. Drawing converts one form to the other by mechanically pulling apart the folded chain crystals and recrystallization in imperfect bundle form. Our structure analysis work described in part 1 clearly indicates, that this interpretation cannot be correct at least for the case of the PET samples. It may also be mentioned that in contrast to Bell and Dumbleton[12] the first peak (low temperature) has been interpreted by Roberts[10] as being due to bundle-like crystals and $T''_m$ due to chain folded crystals.

We suppose that according to Holdsworth *et al.*[11] the position of the melting peak is not directly related to the structure of the material before scanning but due to a competition of recrystallization and melting. Then the question arises for the origin of the differences between drawn and undrawn material. Here one has to take into account, that the fusion curves of *Figures 1* and *2* are obtained from samples which have been annealed for constant times at the indicated annealing temperature. On the other hand it has been shown for undrawn PET[10,11] and polyamide-6 [5] that increasing annealing time qualitatively has the same effect as increasing annealing temperature, i.e. $T'_m$ moves to higher temperatures and $\Delta H'$ increases at the expense of $\Delta H''$. So both crystallization temperature and crystallization time determine the shape of the fusion curve. Long annealing times have the effect of increasing the free enthalpy of the original crystallites and so shifting the melting point $T'_m$ to higher temperatures.

In drawn PET the $T'_m$ has rather high values already for

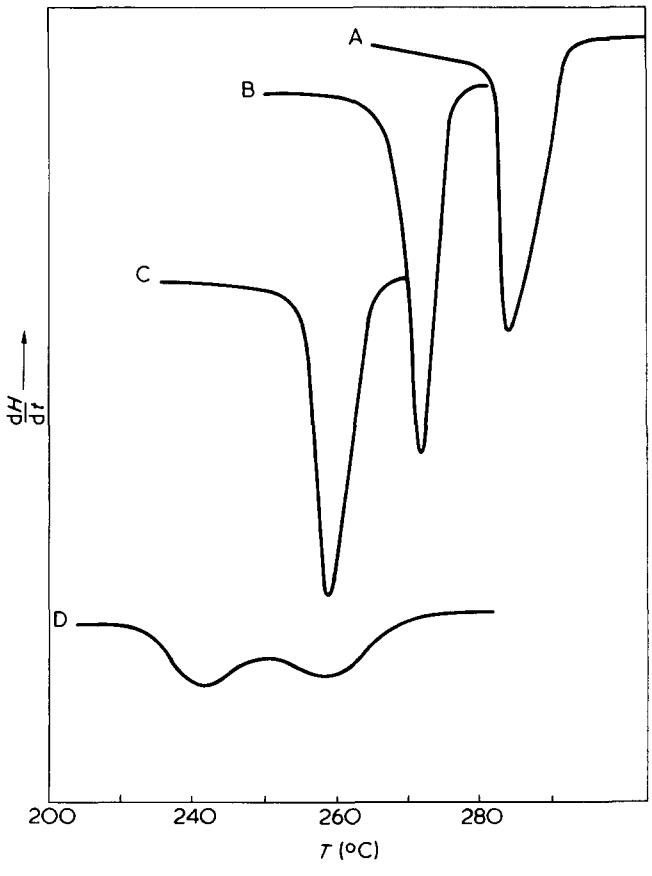


*Figure 6* D.s.c. thermograms for drawn PET bristles annealed at 240°C for various times; A, 10 000 min; B, 1000 min; C, 100 min; D, 10 min

shorter annealing times. One has to take into account, however, that the crystallization kinetics is completely different for drawn and undrawn material. It has been demonstrated[13] that drawn PET crystallizes much faster than undrawn samples. Therefore the same annealing time in the two cases may result in a quite different behaviour. It seems reasonable to suppose that the fusion curve of drawn material after a certain annealing time represents just the fusion curve of an undrawn sample after a much longer annealing time. Accordingly in the case of a drawn sample a double fusion peak should appear after rather short annealing times. This is observed as demonstrated by *Figure 6*. Even for an annealing temperature as high as 240°C, two endothermic peaks appear after a short annealing time (10 min), whereas longer annealing leads to one peak only*. So our conclusion is that the differences in the melting behaviour of undrawn and drawn PET is caused by the different crystallization kinetics in so far as a given annealing time for the drawn state corresponds to a much longer annealing time in the undrawn state.

*Degree of crystallinity of drawn poly(ethylene terephthalate)*

As was pointed out in part 1 of our work the evaluation of the degree of crystallinity of drawn PET samples from density values causes serious difficulties since the application of the conventionally employed 'two-phase model' leads to inconsistent data. Usually the volume fraction $w_c$ of the crystalline phase is calculated form the measured density $\rho$ by the equation:

$$w_c = \frac{\rho - \rho_a}{\rho_c - \rho_a} \tag{4}$$

where $\rho_c$ and $\rho_a$ are the ideal values of the densities of the crystalline and amorphous regions. This procedure comprises the assumptions that the properties of each phase are independent of the amount of the other phase and that the crystalline phase has the structure of a perfect crystal. In the following we will show that these assumptions do not hold in the case of PET and that therefore equation (4) can only be applied if the effective densities $\rho_c^*$ and $\rho_a^*$ are used instead of the ideal values.

The inconsistency of the conventional two-phase model is clearly demonstrated by the following observations: firstly the mean square density fluctuation $\langle\eta^2\rangle_{exp}$ measured by small-angle X-ray scattering is much smaller than the value $\langle\eta^2\rangle_{cal}$ calculated on the basis of a two-phase structure according to the equation:

$$\langle\eta^2\rangle_{cal} = (\rho_c - \rho_a)^2 w_c(1 - w_c) \tag{5}$$

The deviations of the measured quantities from the calculated values are the larger the lower the annealing temperature (see Figure 20 of ref 1). Secondly large discrepancies exist between the crystallinities calculated either from density measurements or from the measured values of the heat of fusion. As shown in *Figure 7* and *Table 2* there are only rather small variations in $w_c$ (d.s.c.), whereas a strong increase of $w_c$ ($\rho$) is observed with rising annealing temperature In the range of annealing temperatures between 140° and 250°C $w_c$ (d.s.c.) changes for about 10%, whereas $w_c(\rho)$ increases as much as 30%.

Although the absolute values of $w_c$ (d.s.c.) are inaccurate to some extent because of the difficulties mentioned earlier, it seems that the general tendency of a rather invariable $w_c$ (d.s.c.) exists in contrast to a large variation of $w_c$ ($\rho$). In addition for lower annealing temperatures the $w_c$ (d.s.c.) values are higher than the $w_c$ ($\rho$) values (see *Figure 7*), in agreement with observations obtained for other polymers; i.e. for drawn polyethylene[4,14].

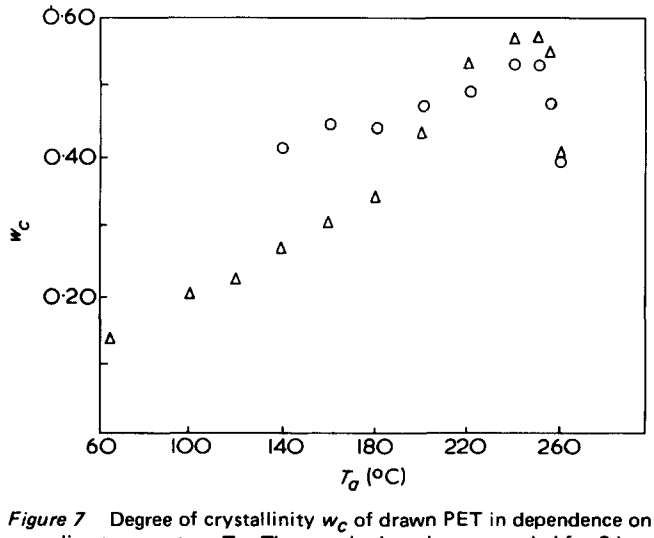


*Figure 7* Degree of crystallinity $w_c$ of drawn PET in dependence on annealing temperature $T_a$. The samples have been annealed for 6 h. ○, Values $w_c$ (d.s.c.) determined from heat of fusion; △, values $w_c$ ($\rho$) calculated from density data

* The fact that for the 10 min curve melting starting below 240°C is believed to be caused by the crystallization at lower temperatures during heating the sample to the annealing temperature.

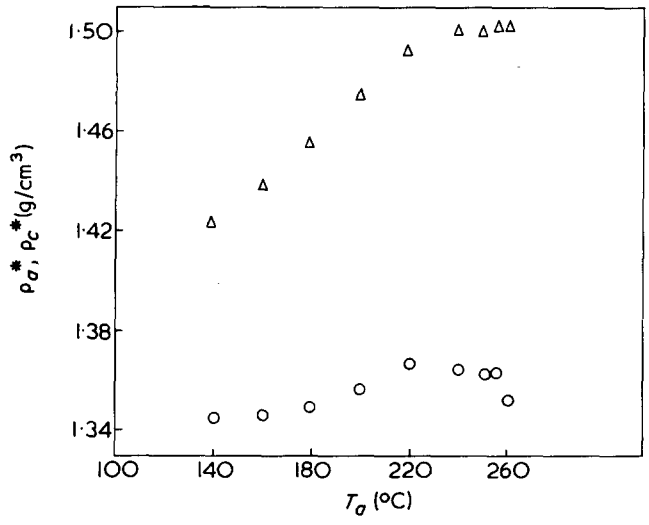


*Figure 8* The effective densities $\rho_a^*$ and $\rho_c^*$ of the amorphous and crystalline regions, respectively, in drawn PET as calculated from the mean square density fluctuation, the average density and the degree of crystallinity $w_c$ (d.s.c )

Two extreme positions can be taken for the explanation of these discrepancies. Either one claims that the enthalpy of the disordered regions $H_{def}$ in the drawn PET has a lower value than the enthalpy of a truly amorphous material or one assumes that the $w_c$ (d.s.c.) values are 'correct' and that the values of $\rho_c$ and $\rho_a$ depend strongly on annealing temperature. Using the first assumption the serious problem of the density fluctuation measured by small-angle scattering is still unsolved. For reasons described in part 1 we adopted the second view and calculated the variation of the effective densities $\rho_c^*$ and $\rho_a^*$ from density, d.s.c. and small-angle scattering measurements. The results are recapitulated in *Figure 8*.

One of the main reasons for this procedure was the sharpening of the wide-angle reflections with increasing annealing temperature $T_a$ (see *Figure 16* ref 1). This effect indicates that the perfection of the crystalline layers in the drawn material depends strongly on $T_a$. Therefore it is reasonable to assume that the effective density $\rho_c^*$ differs from the ideal value of the unit cell of PET and increases with increasing annealing temperature.

The broadening of the crystal reflections observed at lower $T_a$ can either be due to lattice distortions or to crystallite size effects. Starting from the observation, that the net plane spacings are independent of the annealing temperature we concluded in part 1, that the broadening of the reflections is mainly due to a mosaic block structure of the crystalline layers. By the grain boundaries, lattice vacancies are introduced which reduce the effective density $\rho_c^*$. As a consequence a relation should exist between the size of the mosaic blocks and the values of the quantity $\rho_c^*$ plotted in *Figure 8*. Therefore the apparent crystallite size was measured from line broadening.

The dependence of the apparent crystallite dimensions $D$ on the annealing temperature is plotted in *Figure 9*. The values of $D$ were determined as described above. Since lattice distortions have been neglected these data represent only an approximation of the true values of the crystallite size. Nevertheless they can be used for an appraisal of the influence of the mosaic block structure on the apparent density $\rho_c^*$ of the crystalline layer. For this estimation we consider a lamella of thickness $l$ and suppose it is built up by mosaic blocks with dimensions $n_1a$ and $n_2b$ in two directions perpendicular to the chain axes. The simplification of an orthorhombic structure is used, $a$ and $b$ are the unit cell parameters. The specific internal surface:

$$s = \frac{\text{Lateral surface of the grain boundaries}}{\text{Volume of the mosaic blocks}}$$

is given by:

$$s = \frac{n_1a + n_2b}{n_1a \times n_2b} \tag{6}$$

Now we assume that the mosaic blocks are densely packed but that a fraction $m$ of the lattice points in the boundary is not occupied by a molecule. This will lead to relative density defect given by:

$$\frac{\rho_c^{id} - \rho_c^*}{\rho_c} = \frac{(n_1 + n_2)m}{n_1n_2} \tag{7}$$

where $\rho_c^{id}$ is the density of the unit cell and $\rho_c^*$ is the overall density of the lamella. Consequently one obtains:

$$s = \frac{n_1a + n_2b}{(n_1 + n_2)abm} \frac{\rho_c^{id} - \rho_c^*}{\rho_c} \tag{8}$$

With the further approximation $n_1 \sim n_2 \sim \bar{n} = (n_1 + n_2)/2$ the vacancy fraction $m$ can be obtained from:

$$s = \frac{a + b}{2abm} \frac{\rho_c^{id} - \rho_c^*}{\rho_c} \tag{9}$$

In *Figure 10* the specific internal surface $s$ calculated from

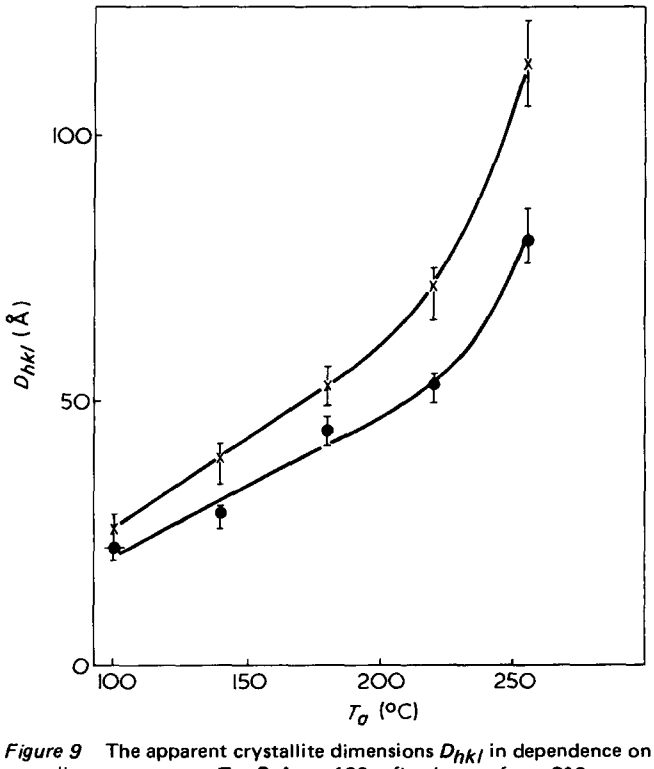


*Figure 9* The apparent crystallite dimensions $D_{hkl}$ in dependence on annealing temperature $T_a$. ●, from 100 reflection; x, from 010 reflection

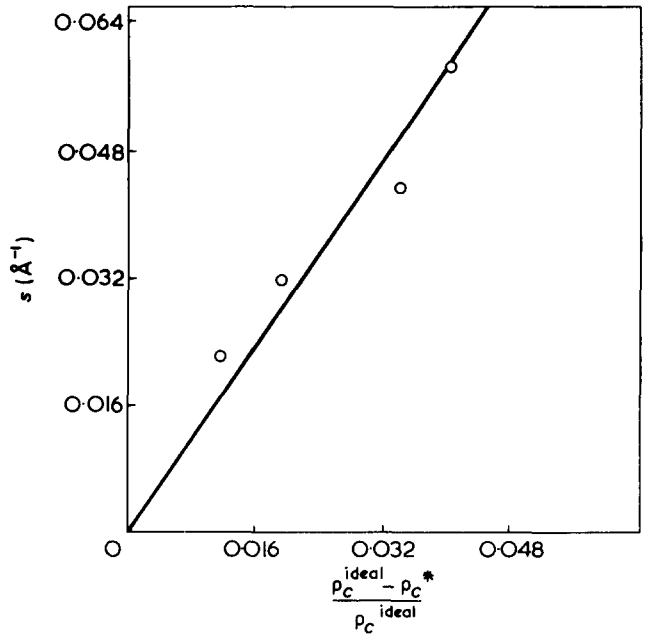


*Figure 10* The specific internal surface $s$ of the mosaic block grains within the crystalline lamella as function of the relative density defect between ideal and effective crystalline densities

the data of *Figure 9* is plotted *versus* the relative density defect which has been determined by small-angle X-ray scattering (*Figure 8*). In good approximation a straight line is observed. From their slope a vacancy fraction $m \sim 14\%$ is calculated. This value may be compared with the relative density difference $(\rho_c^{id} - \rho_a^{id})/\rho_c^{id}$ between crystalline and amorphous PET which is about 12%. So it follows from this analysis that the grain boundary of the mosaic blocks is covered by a layer of amorphously packed molecules

It has to be emphasized that the data used in *Figure 10* originate from quite different sources. The specific surface has been determined from the line shape of the wide-angle reflections, whereas the effective density defect was calculated from the results of density, d.s.c. and small-angle X-ray measurements. So our estimation yields a surprisingly good agreement and supports our previous hypothesis described in part 1. It was concluded that the density of the crystallites is by no means identical with the so-called 'X-ray density' but considerably smaller due to lattice vacancies located at the boundaries of the mosaic blocks. The enthalpy (per gram crystallite) is less effected by the vacancies since the surface energy of the lateral surfaces of the mosaic blocks can be considered to be rather small compared with the heat of fusion.

Neglecting this contribution means, that the values of $w_c$ (d.s.c.) calculated according to equation (1) are somewhat smaller than the real mass fraction of crystalline lamellae (including the grain boundary material). On the other hand in our analysis we have identified $w_c$ (d.s.c.) with the crystalline volume fraction $v^c$, which is given by:

$$v^c = \frac{\rho}{\rho_c} w_c \qquad (10)$$

and is therefore also a little smaller than $w_c$. A rough estimation shows that both corrections are in the same order of magnitude. So they compensate each other and we suppose that the crystallinity calculated from equation (1) is a rather accurate measure of the crystalline volume fraction.

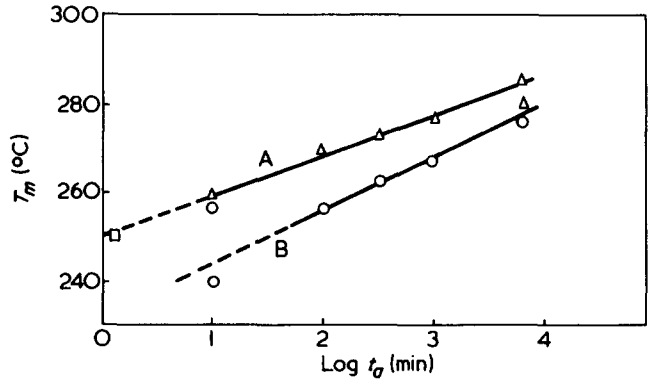


*Figure 11* Effect of annealing time $t_a$ on the melting temperature (from d.s.c.) for drawn PET bristles annealed at: 240°C (○); 255°C (△). Heating rate 10°C/min (□, annealed in oil at 240°C). A, $T''_m$; B, $T'_m$

A general remark about the comparison of density and heat of fusion may be useful. So far as one can be sure that neither $\rho_a$ nor $\rho_c$ nor $(H_c - H_a)$ depend on the crystallization and pretreatment conditions such a comparison leads to reasonable conclusions. It seems that at least in drawn polymers as a rule serious difficulties arise. For example, in drawn polyethylene the enthalpy and the specific volume of the disordered regions are smaller than those for the amorphous regions in isotropic material[4,14]. In the case of PET the main effect is the lower value $\rho_c^*$ of the density of the crystalline layers as it has been shown. For semicrystalline melt-crystallized polymers in the isotropic state a similar situation may exist, especially in such cases where the wide-angle X-ray patterns indicate large changes of the state of order of the crystalline regions depending on crystallization temperature. The influence of incomplete order (either due to crystal distortions or to crystal boundaries) on the density may be quite different from the impact of defects on the enthalpy. A convincing example is the introduction of lattice vacancies.

*Effect of annealing time*

The influence of the annealing time $t_a$ on the melting behaviour of drawn PET samples was also studied. Some of the melting curves have been shown in *Figure 6* for samples annealed at 240°C. Another run was carried out at an annealing temperature of 255°C. The results are plotted in *Figures 11* and *12*. *Figure 11* shows that the apparent melting temperature $T_m$ increases almost linearly with the logarithm of annealing time as was also found in the case of undrawn PET[10]. A double melting peak was only observed at the shortest annealing time† (*Figure 6*).

The melting point and the crystallinity of a sample annealed for 1 min directly in an oil bath were approximately equal to the data for a sample annealed for 100 min *in vacuo* (see *Figures 11* and *12*). Similar effects have been described already by other authors[15] and are due to the extremely rapid crystallization of the drawn PET in the very beginning of the annealing procedure and therefore the heat conduction plays an important role.

The heat of fusion $\Delta H_{exp}$ depends also logarithmically on the annealing time. The corresponding values of $w_c$ (d.s.c.)

† For very long times (10 000 min at $T_a = 255°C$) a small splitting of the single endothermic peak is again observed, probably due to chemical reactions. In addition a decrease of $\Delta H_{exp}$ is found for that time.

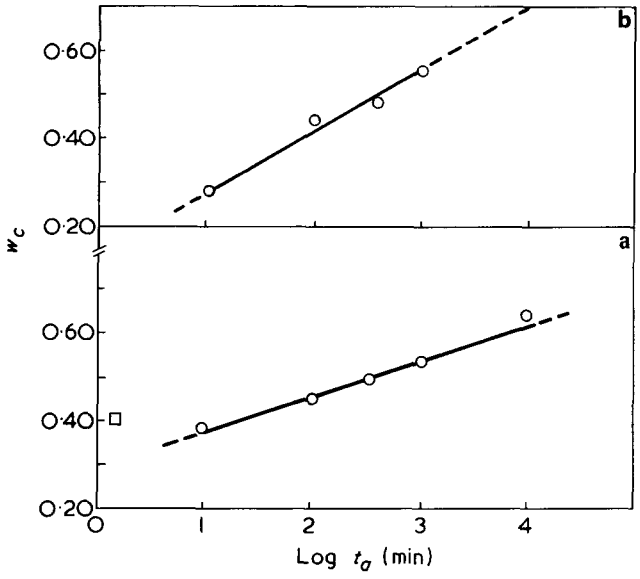


*Figure 12* Effect of annealing time $t_a$ on the degree of crystallinity $w_c$ (d.s.c.) of drawn PET samples annealed at: (a) 240°C (b) 255°C (□, annealed in oil at 240°C)

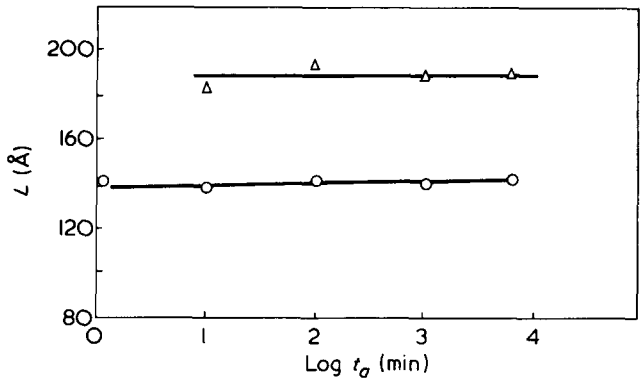


*Figure 13* The long spacing $L$ of drawn PET in dependence on annealing time $t_a$ for two annealing temperatures $T_a$ (The 1 min-sample was annealed in an oil bath). ○, 240°C; △, 255°C

are plotted in *Figure 12*. It is quite clear that prolonged annealing results in an increase of the order of the semicrystalline PET as is well known for many other polymers. Surprisingly the long spacing $L$ measured by SAXS remains almost constant, however, as shown in *Figure 13*. This behaviour is quite different from the generally observed increase of the long spacing $L$ with the logarithm of time[16], which is commonly described as 'isothermal thickening'.

Since both the melting point $T_m$ and the crystallinity $w_c$ increase during annealing it is reasonable to propose that the heat treatment results in a growth of the crystalline layers into the amorphous interlamellar material in the course of which the average distance of the centre of gravity of the crystalline lamellae remains constant. This hypothesis can be checked by plotting the melting point $T_m$ *versus* the reciprocal thickness $1/l$ of the crystalline layer. According to the discussion above the values $w_c$ (d.s.c.) are reasonably good approximations of the crystalline volume fractions and so $l$ is given by:

$$l = Lw_c \tag{11}$$

As shown in *Figure 14* one obtains a straight line and from

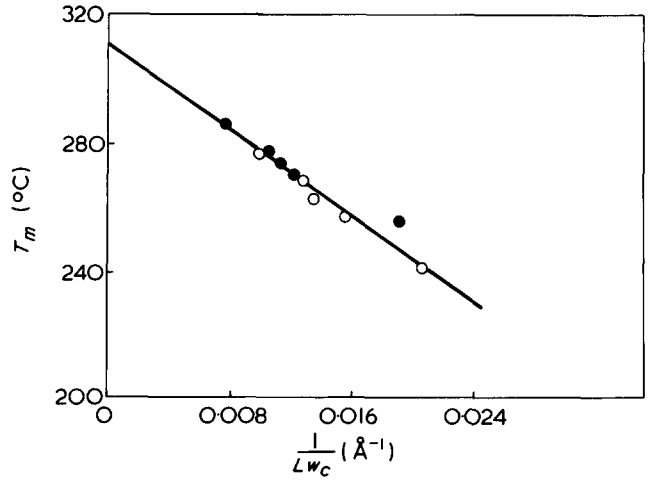


*Figure 14* Relationship between the melting temperature $T_m$ (from d.s.c.) and the crystallite size $l = Lw_c$ for drawn PET samples annealed at constant temperature for various times: $T_a$ = 240°C (○); $T_a$ = 255°C (●)

the well known equation:

$$T_m = T_m^\infty \left(1 - \frac{2\sigma_e}{\Delta H^0 l \rho_c}\right) \tag{12}$$

the melting point $T_m^\infty$ of the infinite large crystal and the surface energy $\sigma_e$ of the longitudinal surface can be estimated. The evaluation yields $\sigma_e \sim 55$ erg/cm$^2$ and $T_m^\infty \sim 310$°C. The first value is in the range reported for other polymers[17] and seems to be acceptable. Consequently the equilibrium melting point $T_m^\infty$ is considerably higher than commonly assumed[18]. Superheating effects[19] may play some role, but since the heating rate was rather slow (10°C/min) these effects may result in a shift of only about 5°C to lower temperature‡

With regard to the influence of annealing time, two questions arise: the observation of constant long spacings is in contrast to the behaviour of undrawn PET, where a decrease of $L$ with time was found[20]. One may suppose that during annealing the staggering of the chains is improved and that therefore the intensity distribution along the layer line in the small-angle pattern is changed in direction to a four point diagram. Isotropic averaging will lead to an apparent decrease of $L$. Studies are underway to prove this assumption.

The second important question concerns the origin of the differences between PET and many other polymers regarding the isothermal thickening process which is related to the so-called 'secondary crystallization'. The increase of long spacing during the crystal thickening requires a complete reorganization of already existing crystallites. Several models have been proposed for this process[21], especially in the case of polyethylene. The different behaviour of PET indicates that the reorganization is extremely handicapped and that the crystals can only grow at the expense of the neighbouring amorphous layer. A similar behaviour was observed in the case of polyamide-6 and explained along the same line[5]. One may speculate that the hindrance of the long spacing increase is the reason for the relatively low ultimate crystallinity of PET and polyamide-6 crystallized under conventional conditions, since the thickness of the amorphous layer cannot pass a certain lower limit.

‡ There may also be some effects caused by chemical changes[19] but their influence is hard to estimate at the present time.

The growth of the crystal into the amorphous layer and the subsequent increase of melting temperature establish again our suggestions on the origin of the double melting endotherms. With increasing annealing time the first peak $T'_m$ should move to higher temperatures as it has been observed[10,11]. As was pointed out by Illers[22] a third endothermic peak at low temperatures may exist, which does not move during annealing or change of the scanning rate. So the melting behaviour of PET may be even more complex as described above. In addition the polycondensation reactions taking place during annealing may also influence the physical behaviour. These unsolved problems complicate the molecular interpretation of the origin of the structures and properties which we described.

## CONCLUSIONS

(a) For the appearance of the double melting peaks in the d.s.c. curves of undrawn PET we accept the explanation by Holdsworth *et al.*[11] that crystallites formed at low temperatures melt and recrystallize with the higher perfection during the d.s.c. scan. The apparent differences between drawn and undrawn samples – annealed for the same times – can be easily explained by taking into account the effects of annealing time and crystallization rate. Drawn PET shows a melting behaviour like an undrawn sample annealed for much longer times.

(b) The crystalline layers have an effective density $\rho_c^*$ which is considerably lower than the ideal X-ray density $\rho_c^{id}$. The density defect $(\rho_c^{id} - \rho_c^*)$ is due to lattice vacancies caused by the grain boundaries of the mosaic blocks. This model proposed already in part 1 has been confirmed by comparing the apparent crystallite sizes in a direction perpendicular to the chains with the density defect $(\rho_c^{id} - \rho_c^*)$. It turned out that in the average the PET packing density at the lateral grain surface is equal to that of amorphous PET.

(c) The degree of crystallinity $w_c$ (d.s.c.) calculated from the heat of fusion is the relevant quantity for describing the volume fraction of crystalline material and more suitable than $w_c$ ($\rho$) calculated from density measurements.

(d) During annealing of drawn PET crystal thickening occurs without an increase of long spacing $L$. This observation indicates that once formed crystallites cannot be reorganized during the annealing treatment in contrast with other polymers like polyethylene. The hindrance of reorganization may be the reason for the relatively low ultimate crystallinity of PET.

## ACKNOWLEDGEMENTS

This work was supported partly by the 'Sonderforschungsbereich 41 der Deutschen Forschungsgemeinschaft' and partly by the 'Alexander v. Humboldtstiftung'. The PET was kindly supplied by BASF, Ludwigshafen. We also wish to thank Dr K. H. Illers, Ludwigshafen, and Dr J. H. Wendorff, Mainz, for helpful discussions. One of us (E.W.F.) appreciates the hospitality of the Department of Physics, University of Leeds.

## REFERENCES

1 Fischer, E. W. and Fakirov, S. *J. Mater. Sci.* 1976, **11**, 1041
2 Wunderlich, B. 'Macromolecular Physics', Academic Press, New York and London, 1973, Vol 1, p 389
3 Dole, M. *J. Polym. Sci.* 1956, **19**, 347; Smith, C. W. and Dole, M. *ibid*, 1956, **20**, 37; Kirshenbaum, I. *J. Polym. Sci. (A)* 1965, **3**, 1869; Slade, P. E. and Orofino, T. A. *Polym. Prepr.* 1968, **9**, 825
4 Fischer, E. W. and Hinrichsen, G. *Kolloid Z. Polym.* 1966, **213**, 93
5 Illers, K. H. and Haberkorn, H. *Makromol. Chem.* 1971, **142**, 31
6 Illers, K. H. *Angew. Makromol. Chem.* 1970, **12**, 89
7 Klug, P. and Alexander, L. E. 'X-ray Diffraction Procedures for Polycrystalline and Amorphous Materials', 2nd Edn, New York–London, 1974, 689
8 Hosemann, R. and Wilke, W. *Faserforsch. Textiltech.* 1964, **15**, 521
9 Yubayashi, T., Orito, Z. and Yamada, N. *J. Chem. Soc. Jpn* 1966, **69**, 1798
10 Roberts, R. C. *Polymer* 1969, **10**, 117
11 Holdsworth, P. J. and Turner-Jones, A. *Polymer*, 1971, **12**, 195
12 Bell, J. P. and Dumbleton, J. H. *J. Polym. Sci. (A-2)* 1969, **7**, 1033
13 Smith, F. S. and Steward, R. D. *Polymer* 1974, **15**, 283
14 Peterlin, A. and Meinel, G. *J. Appl. Phys.* 1965, **35**, 3028
15 Dumbleton, J. H. *Polymer*, 1969, **10**, 539
16 Fischer, E. W. and Schmidt, G. F. *Angew. Chem.* 1962, **74**, 551
17 Hoffman, J. D., Davis, G. T. and Lauritzen, F. I. in 'Treatise on Solid State Chemistry', (Ed. N. B. Hannay), Plenum Press, New York, Vol. 3, 1976
18 Brandrup J. and Immergut, E. H. 'Polymer Handbook', Interscience, New York, 1969
19 Miyagi, A. and Wunderlich, B. *J. Polym. Sci.* (A-2), 1972, **10**, 1401
20 Zachmann, H. G. and Schmidt, G. F. *Makromol. Chem.* 1962, **52**, 23
21 Fischer, E. W. *Pure Appl. Chem.* 1972, **31**, 113
22 Illers, K. H. personal communication